Journal of Thermal Analysis and Calorimetry
https://doi.org/10.1007/s10973-024-13555-0

Study on optimizing the energy gradient and temperature regulation of flat plate solar collectors with advanced hybrid nanofluids

M. Arulprakasajothi[1] · A. Saranya[2] · B. Srimanickam[3] · Yuvarajan Devarajan[4] · N. Dilip Raja[5]

Received: 1 June 2024 / Accepted: 3 August 2024

Abstract

The objective of this research study is to enhance the performance of a flat plate collector by using various cooling fluids, as an increase in solar panel temperature can decrease its efficiency. The experiment utilized three different fluids: distilled water, zinc sulfide nanofluid, and copper zinc sulfide nanofluid. FTIR analysis revealed a pronounced peak at 1133 cm^{-1}, indicating the presence of Cu^{2+} ions in ZnS. Three key parameters were systematically examined to optimize the solar panel's energy gradient and temperature variance. The flow rate of the cooling fluid varied from 0.5 to 2.0 L min^{-1}. Notably, the use of copper zinc sulfide nanofluid resulted in improvement in the energy gradient, reaching a peak value of 1112 W m^{-2}. The temperature difference showed a significant increase, peaking at 4.73 °C when using CuZnS nanofluid at a flow rate of 1.5 L min^{-1}. The incorporation of copper particles in the nanofluid notably enhanced the thermal conductivity of the cooling fluid. This improvement significantly boosted the efficacy of heat transfer processes, thereby increasing the overall efficiency of the solar panel system.

Keywords Nanofluids · Solar power · Renewable energy · Sustainable practices · Environmental sustainability

Introduction

The demand for technologies to create alternate energy generation methods is growing as fossil fuels are predicted to run out before the turn of the century. The quantity of solar energy, specifically solar PV and solar thermal, has demonstrated enormous potential to compete with fossil fuels and eventually replace them in the production of electricity. Solar panels collect light energy in the form of thermal energy, which can have an impact on their performance and lifespan. Thermal energy is vital in working typical systems in any given scenario. Typical gadgets are designed to operate in an ideal environment. However, during the actual use of the gadgets, they are used in dynamic environments that significantly increase the operating temperatures. The dynamic nature of the operating environment affects the effectiveness of the gadgets. In some cases, the temperature can be very low; in others, the atmosphere can be too hot. In either case, the gadgets seldom operate in an ideal environment. Delouei et al. investigated ways to improve heat transfer in indirect water bath heaters as well as the augmentation of heat transfer in indirect heaters using an active method in experimental modelling [1]. As a result, the elimination panel may be cooled using a variety of methods, including air, water, and nanofluids based on water. Air, on the other hand, has a limited ability to transfer heat; therefore, water and water-based nanofluids can remove heat from the back of the solar panel more effectively. As a consequence, the flat plate solar collector's performance has significantly improved. Further, water-based nanofluids have been produced better result than conventional fluids.

✉ Yuvarajan Devarajan
dyuvarajan2@gmail.com

[1] Department of Mechanical Engineering, Centre for Thermal Management, KCG College of Technology, Karapakkam, Chennai 600 097, India

[2] Department of Physics, Centre for Thermal Management, Veltech Rangarajan Dr. Sagunthala R&D Institute of Science and Technology, Chennai, Tamil Nadu 600062, India

[3] Department of Mechanical Engineering, Centre for Sustainable Energy, Jaya Engineering College, Thirunindravur, Chennai, Tamil Nadu 602 024, India

[4] Department of Mechanical Engineering, Saveetha School of Engineering, SIMATS, Savetha University, Chennai, Tamil Nadu, India

[5] Department of Mechanical Engineering, Veltech Rangarajan Dr Sagunthala R&D Institute of Science and Technology, Chennai, Tamil Nadu 600062, India

Published online: 03 September 2024

A flat plate solar collector and an evacuated tube solar collector are two types of solar collectors. It is possible to combine two power conversion systems to increase productivity, which are called hybrid or photovoltaic thermal systems [2]. There are many benefits to using solar energy, including its free nature, feasibility, durability, low maintenance cost, and environment-friendly nature [3]. However, it has some drawbacks, such as increasing the solar panel's temperature by 10 Celsius, resulting in a 0.5% decrease in electrical efficiency for silicon panels since cooling may be required. Cooling liquids such as air or water are used to decrease the temperature of solar panels [4]. There are two ways to improve the performance of a solar panel. Firstly, solar panel cooling is a means of storing waste heat. Solar panels are traditionally cooled by air and water [5]. Despite this, it has some virtues and merits of its own. Due to the above encounters, researchers worldwide have utilized nanomaterials to enhance thermal and electrical performance [6]. In turn, this can improve overall performance. The following are some successful studies conducted worldwide; due to their better thermophysical properties than standard fluids, Choi and Estman [7] introduced nanofluids as a cooler in PVT systems. In nanofluids, nanoparticles drift in water with diameters ranging from 1 to 100 nm in company with solids [8].

When compared to essential fluids, water nanofluid has a significantly higher heat transfer coefficient [9]. However, there are a few weaknesses in using nanofluids in hybrid collectors [10], such as the enhanced pressure drop of the system [11] Alami et al. used a unique form of channel box PVT collector to study a number of factors, including solar irradiations, temperature of solar PVT collectors, electrical efficiency, electrical power, and overall efficiency. [12], and the high cost of nanoparticles. PVT systems were tested using water as a base fluid, SiO_2 nanofluid, and various concentrations of SiO_2 nanofluid by Sardarabadi et al. 2014 [13]. Compared with PVT water, total performance was achieved at 3.6% for 1 mass% and 7.9% for 3 mass%. Ghadiri et al. 2015 [14] analyzed water and ferrofluids of varying compositions with an indoor PVT system. This approach was 45% more efficient than a hybrid—deionized water containing 0.2 mass% of three kinds of nanoparticles (Al_2O_3, TiO_2, ZnO) were presented by Sardarabadi et al. 2016 [15]. Various nanofluids were experimented with at a variety of flow rates by Al-shamanic et al. 2016 [16]. As a result, SiC had the highest electrical efficiency of 78.24% and the highest electrical performance of 13.52%. A hybrid water nanofluid system was investigated by Soltani et al. 2017 [17]. The study found that total enactment increased by 3.13%, and power generation increased by 52.4% as a result found that using SiO_2 enhanced actual performance and power generation by 3.29 and 43.36%, respectively. The experimental investigation of three types of water-based nanofluids by Al-Waeli et al. 2017a [18] was carried out using collectors.

Silicon chloride/water nanofluid, Al-Waeli et al. 2017b [19] enhanced the electrical efficiency of the hybrid system to 23.9% and the heat power efficiency to 99.23%, it found a superior overall performance compared to a PV system of about 88.9% and the result found that 7.9% and 24.3% were gained in overall efficiency and exergy, respectively. To ensure long-term stability, Ag/water nanofluids were processed by electrical wire explosion [20]. Yuhui [21] studied solar thermal energy collection using a flexible composite phase change material derived from genetically modified wood. This approach resulted in stability and durability surpassing typical levels. They also investigated the material's flame-retardant properties, electromagnetic shielding, and thermal-to-electricity conversion capabilities. Valiyollah [22] utilized computational fluid dynamics to examine the impact of nanofluids on heat exchanger performance. They conducted several parametric simulations, exploring various flow rates, outlet temperatures, heat transfer factors, and pressure drops. Their findings revealed that using nanofluids significantly improved heat exchanger efficiency, offering notable benefits for various industrial applications. A thermodynamic study of the system was conducted to assess its energy and exergy efficiency. An experimental study was conducted with different concentrations and flow regimes. Photovoltaic/thermal collectors have been investigated extensively for improved performance with nanofluids. Several studies have demonstrated that nanofluids can be used as operational fluids in solar collectors to boost their thermal efficiency. By increasing nanoparticle concentrations within the nanofluid, notable improvements in collector efficiency can be achieved [23]. Nanoparticles distributed within heat transfer fluids have shown greater efficacy than integrating them into phase change materials in enhancing the performance of photovoltaic/thermal systems [24].

Solar collector performance and thermal efficiency can be enhanced by optimizing key nanofluid attributes, including thermophysical characteristics and stability [25]. In addition, nanofluids have been demonstrated to enhance PV solar panel efficiency compared with non-cooled PV systems and water-based cooling methods [26]. Nanofluids are becoming more popular than traditional cooling technologies due to their superior thermal conductivity and heat transfer characteristics. By suspending nanoparticles in base fluids such as water, nanofluids significantly enhance the thermal performance of cooling operations. This improved efficiency is especially vital in applications requiring precise temperature regulation and effective heat dissipation, such as in electronics, automotive, and industrial cooling systems. Furthermore, nanofluids can be specifically engineered to enhance particular properties, such as viscosity and thermal conductivity, offering a flexible and adaptable solution suitable for diverse requirements. By improving the efficiency of heat transfer systems, nanofluids contribute to sustainability objectives, reducing energy consumption and mitigating greenhouse gas emissions. As a promising alternative to traditional cooling methods, nanofluids can help protect the environment and advance the development of sustainable technologies.

Nano-based cooling systems, such as nanofluids and nano-enhanced phase change materials (PCMs), have significantly improved PV efficiency. The use of hybrid photovoltaic thermal systems for cooling and improving PV panel efficiency has also been demonstrated [27]. The use of hybrid photovoltaic thermal (PVT) systems has also been demonstrated as an effective approach for cooling and enhancing the efficiency of PV panels. These systems integrate photovoltaic cells with thermal collectors, allowing for the simultaneous generation of electrical and thermal energy. By using a fluid medium, such as water or air, to absorb excess heat from the PV cells, PVT systems can significantly reduce the operating temperature of the panels. This cooling effect not only prevents efficiency losses due to overheating but also harnesses the extracted thermal energy for various applications, such as water heating or space heating. Consequently, PVT systems offer a dual benefit of improved electrical efficiency and additional thermal energy production, making them a promising solution for maximizing the overall energy output of solar installations. These systems combine solar panels with solar thermal absorbers. Thermoelectric cooling, water circulation, water immersion, and heat sinks are also employed [28]. Despite its drawbacks, such limited efficiency and high installation costs, solar energy is a free and ecologically beneficial energy source. Additionally, because it is entirely dependent on sunshine, it is defined as an intermittent renewable and partially continuous source. Further, among the most important clean energy sources that are renewable, solar energy is widely available [29]. Copper-zinc sulfide (CuZnS) nanoparticles mixed with water are used as a coolant to improve the performance of PVT collectors. To the author's knowledge, CuZnS nanofluid has been experimentally investigated for the first time, cooling and improving the performance of a single-glazing surface PVT system. An experimental procedure was setup near Chennai in Avadi, Tamil Nadu, using a PVT collector with serpent-type heating elements. The designed PVT collector and PV module were tested outdoors in the Chennai meteorological station at 0.5 and 1.0 L min^{-1} rates with nanofluids and purified water as coolants. A comparison of hybrid collectors with nanofluid coolants with PV modules and water-cooled PVT systems was conducted. A comparison was also made between the results of this study and those published in the scientific literature. The study helps to determine the influence of ceramic nanofluids and metallic nanofluids on the performance improvement of solar panels.

This research investigates enhancing flat plate collector performance through the use of various cooling fluids to mitigate the performance decrease caused by rising solar panel temperatures. The study evaluates distilled water, zinc sulfide nanofluid, and copper zinc sulfide nanofluid, employing Fourier transform infrared (FTIR) analysis to identify doping ions in ZnS. By optimizing parameters such as cooling fluid flow rate (ranging from 0.5 to 2.0 L min^{-1}), it is discovered that the CuZnS nanofluid significantly improves thermal conductivity and heat transfer, resulting in a peak energy gradient of 1112 W m^{-2} and a temperature difference increase to 4.73 °C at a flow rate of 1.5 L min^{-1}. This study uniquely evaluates the efficiency enhancement of a flat plate solar collector using advanced nanofluids, particularly focusing on copper zinc sulfide (CuZnS) nanofluids. The presence of Cu^{2+} ions in ZnS significantly improves thermal conductivity, optimizing cooling performance. The CuZnS nanofluid achieved an impressive energy gradient of 1112 W m^{-2} and a temperature difference of 4.73 ℃, highlighting its superior effectiveness. This research advances the understanding of innovative cooling methods for sustainable energy systems.

Materials and methods

The increasing pollution of the environment and the need for more energy highlight the importance of developing renewable energy sources, particularly solar photovoltaic (PV) panels. While PVs are recognized as eco-friendly and long-lasting energy solutions, their conversion efficiency is relatively low, typically between 15 and 20%. Most incident sunlight is absorbed as heat rather than converted into electricity. This elevated surface temperature adversely affects PV panels' efficiency and reliability [30, 31]. Therefore, finding an effective cooling method is crucial to enhancing PV performance. Heat accumulation can be mitigated by a suitable cooling technique, improving conversion efficiency and reliability overall.

Experiments were carried out in Avadi, a city in Tamil Nadu in the southern part of India that serves as the capital. The study site was at 13.0827° N latitude and 80.2707° E longitude. Chennai had a tropical wet-dry summer and a dry climate according to Köppen's Climate Classification [32]. Located on the thermal equator and along the coast, the city's geographical location has moderate seasonal temperatures. This region has an average relative humidity of 69%. With an average of eight hours (approx.) of moderate sunshine, temperatures fluctuate between 24.8 and 33.1 °C. In addition to providing valuable insight into the external factors influencing the study's results, these climatic conditions define the context in which the experiments were conducted.

Experimental investigation

The experiment is carried out to find the effectiveness of cooling fluid in controlling the surface temperature of the solar photovoltaic panel (SPC) when operated for 24 h. The energy gradient and the temperature difference between the SPC and cooling fluid were assessed.

A systematic experimental arrangement was employed to evaluate the temperature disparity between the cooling fluid and the solar panel collector (SPC). The fluid's temperature was precisely measured before and after passing through the SPC by strategically placing thermocouples at the inlet and outlet of the cooling fluid channel. Additionally, surface temperature sensors were attached to the SPC to monitor its temperature at various locations. The temperature readings from both the thermocouples and surface sensors were continuously monitored and recorded using a data acquisition system, while the cooling fluid was circulated at controlled flow rates ranging from 0.5 to 2.0 L min^{-1}. The flow rates of 0.5–2.0 L min^{-1} were selected for several reasons. Firstly, these flow rates are commonly used in practical applications of solar panel cooling, providing a realistic range for evaluating the performance of various cooling fluids. Secondly, this range allows for a comprehensive examination of the correlation between heat transfer efficiency and flow rate. Flow rates as low as 0.5 L min^{-1} can determine the minimum fluid velocity necessary for effective cooling, while flow rates as high as 2.0 L min^{-1} can demonstrate the maximum cooling efficacy achievable without causing excessive pressure drops or mechanical stress in the system. Additionally, this range ensures that the cooling system operates safely and optimally, preventing potential issues such as fluid overflow or inadequate cooling. By analyzing a spectrum of flow rates, the study aims to identify the most effective and efficient flow rate for enhancing the thermal performance of the solar panel collector. The heat transfer efficiency and effectiveness of the cooling fluids were determined by comparing the average surface temperature of the SPC with the average temperature of the cooling fluid at the inlet and outlet. Consequently, the temperature difference was computed accurately.

Three different cooling fluids, i.e., distilled water, water mixed with 0.2 vol. % of ZnS nanoparticles (23 nm size), and water mixed with 0.2 vol. % of CuZnS nanoparticles (18 nm size), were used in this study [33]. In this study, the mixture of nanoparticles and distilled water is termed nanofluid. A comprehensive comparison was conducted between this SPC system operated with and without cooling fluids. The experiment explored the use of water as a cooling agent within the PVT system, varying the flow rate. Four different flow rates, i.e., 0.5 L min^{-1}, 1 L min^{-1}, 1.5 L min^{-1}, and 2 L min^{-1}, were considered for this experiment—furthermore, the effectiveness of the cooling fluid.

Figure 1 illustrates the actual experiment models used in this study. An experimental setup is meticulously detailed in Fig. 2, with a schematic representation. Using these visual aids, a deeper understanding of the operational context and the physical manifestation of the research can be obtained. A multi-silicon glass panel measuring 1640 mm × 992 mm × 35 mm was acquired to construct the photovoltaic thermal collector. On the rear of the solar panel, 0.4-mm copper sheet was used to absorb heat due to the insulation effect of the platform. Additionally, the copper tube is used as a heat absorber from the rear side of the solar panel with a diameter of 1.0 cm externally and 0.8 cm internally.

Fig. 1 Photographic depiction of the experimental procedure

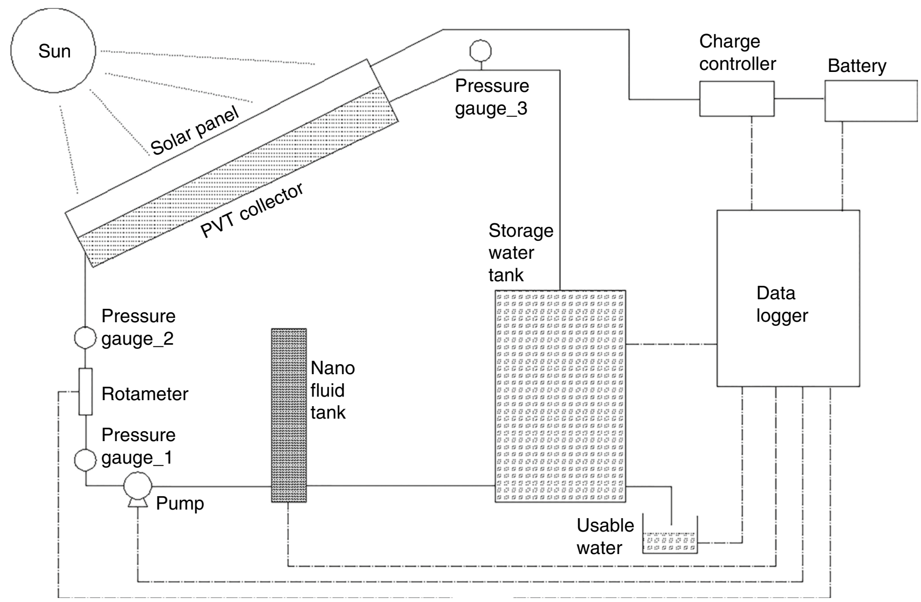

Fig. 2 Schematic view of the tested study

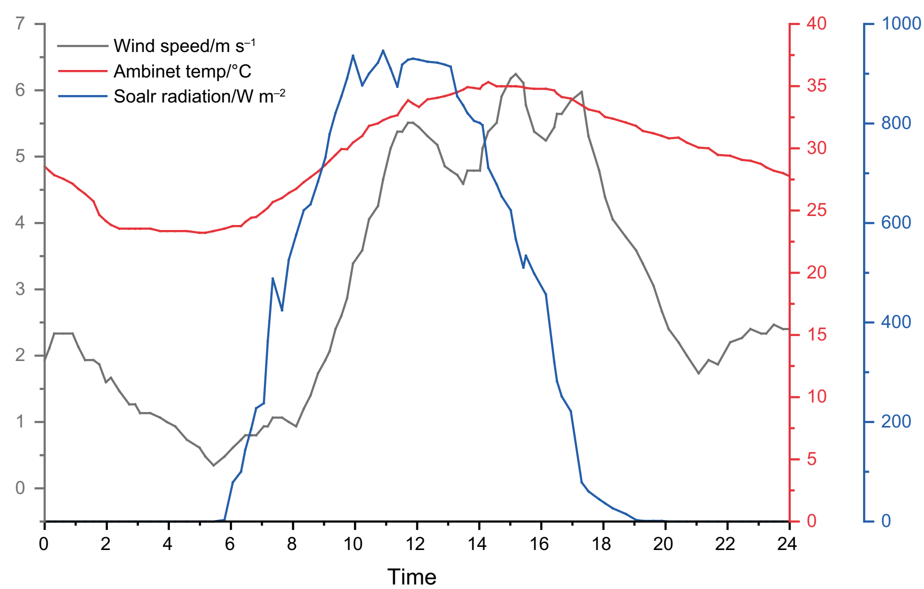

Fig. 3 Ambient condition during the experiment

Figure 3 shows the atmospheric conditions observed during the experiment. The solar radiation was recorded from 05:45 to 17:00. The wind speed fluctuated throughout the experiment. The ambient temperature varied between 23.5 and 35 °C due to atmospheric conditions. Table 1 shows the solar panel's performance based on the typical test settings. In this solar thermal system, the photovoltaics were mounted at an angle of 13° to the south hemisphere. A fifteen-minute reading was from 00:00 to 24:00. In the SPC system, nanofluid coolant was used to increase heat transmission and reduce material costs. Therefore, it is essential to choose competent drivers at reasonable prices that may be sold together as a package. Three parts of the system can

Table 1 Performance of solar panels at the standard test conditions

Parameter	Value
P max	260 W
Amps in Pmax	8.42 A
Volts in Pmax	30.9 V
Current in maximum load	8.89 A
Voltage in maximum load	37.7 V
Mass	1.85 kg

be separated: the collector, the system supporter, and the standalone system.

Synthesis of the nanofluid

The co-precipitation method synthesized zinc sulfide (ZnS) nanocomposites, zinc sulfide, and copper (ZnS: Cu) nanocomposites. Deionized water was used as the reaction medium. Zn acetate dihydrate $(CH_3\ COO)_2$ solution was a typical experiment. Deionized water was dissolved in hydrogen at room temperature an equimolar solution of sodium sulfide non-hydrate $Na_2S.\ 9H_2O$ was prepared in the same reaction medium. Zinc acetate was completely dissolved in the deionized water after vigorous mechanical stirring at 700 rotating per minute (rpm). This was followed by 30 min of stirring the solution. The metal precursor solution was added drop-wise with an equimolar sodium sulfide solution [34]. A milky mixture formed when sodium sulfide solution was added, indicating the formation of zinc sulfide nanoparticles, as shown in Fig. 4. According to earlier research, it was determined to use a certain nanofluid flow rate. This might be utilized in the testing configuration for that specific day's entire experimental setup. All the chemicals employed in the study were of analytical quality and were not further refined. In this work, the nanofluids were created using the two-step approach, which is a method of dispersing nanoparticles in a fluid. After mixing for two hours, the mixture was cooled. Centrifugation was used to collect the white precipitates of zinc sulfide, which were washed three times with distilled water and ethanol. We collected the washed precipitates in crucibles and dried them at 80 °C. We subsequently grained them using a monitor pistol for an hour. The grained powder was collected. The CuZnS nanocomposites were prepared by adding 0.1 M of 100 mL copper acetate solution drop-wise to 0.3 M of zinc sulfide solution for 2 h. To remove residual salts, the precipitate was centrifuged with distilled water and finally with ethanol and then dried at 80 °C in an oven [35]. A similar procedure was used to synthesize ZnS nanoparticles respectively.

Sedimentation

Sedimentation is a significant obstacle in systems that involve nanoparticles. The settling of nanoparticles from suspension can result in decreased efficiency and blockage in heat exchangers, hence greatly reducing the overall performance of the system. It is essential to address this issue in order to preserve the efficacy of nanofluids in thermal applications. Several approaches have been investigated to reduce sedimentation, such as employing surfactants, stabilizing chemicals, and mechanical agitation. Although attempts have been made, sedimentation continues to be an ongoing issue, requiring creative solutions to guarantee the enduring stability and effectiveness of nanofluids.

The use of ultrasonic vibrations is an innovative method to improve heat transmission and decrease sedimentation in heat exchangers that work with nanofluids. Ultrasonic waves generate high-frequency oscillations that efficiently scatter nanoparticles, avoiding their sedimentation and ensuring a consistent suspension. This method has demonstrated considerable potential in enhancing the thermal conductivity of nanofluids, resulting in more effective heat transfer. The utilization of ultrasonic vibrations is a developing area with significant promise for diverse practical applications. It presents a possible solution to the problem of sedimentation and improves the overall performance of systems that use nanofluids.

Uncertainty analysis

Understanding uncertainties is essential for confirming the accuracy of each experimental setup. Among the various

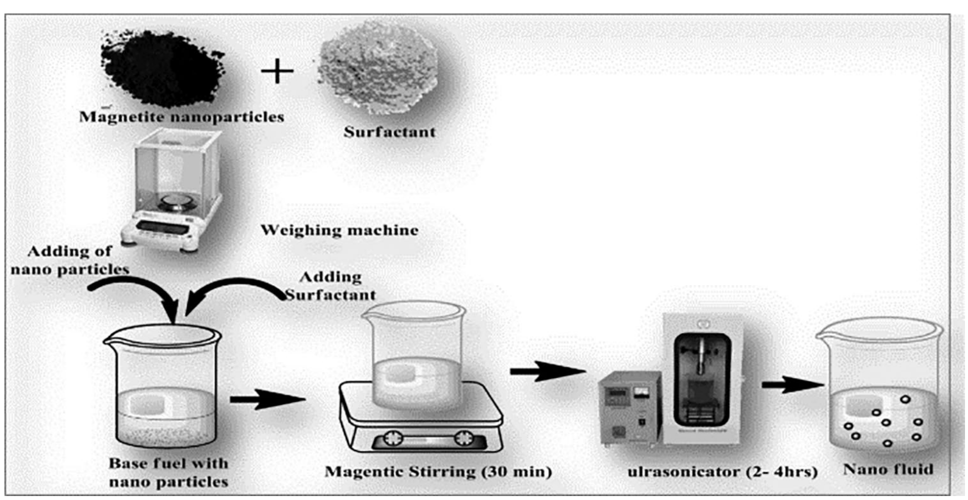

Fig. 4 Synthesis of the CuZnS Nanofluid

Table 2 Individual calibration distortion parameters for the PVT collector

Sensor	Distortion	Type
Ambient air temperature	± 0.2 °C	K-thermocouple
Heat pipe temperature	± 0.2 °C	K-thermocouple
Rotameter	± 2.3%	UKL
Solar power meter	± 4 W m^{-2}	TM-206
Inlet & outlet temperature	± 0.2 °C	K-thermocouple
Data logger	± 3.4%	Agilent 34980A

types of errors are data extraction, calibration, data processing, and ambiguities in specific instruments. Temperature, solar irradiance, stress, and fluid velocity were all extreme measurements in this study, which caused most errors. As can be seen in Table 2, there are individual calibration distortion parameters for the PVT collector. There is a significant uncertainty of around 3.4% in estimating solar collector efficiency (Table 3).

Optimization study on the solar panel

Optimization was carried out using ANOVA and Design Expert V13. Three different parameters, i.e., time of the day, cooling water type, and flow rate of the cooling water in L min^{-1}, were considered as the input parameters for this study. Two different responses, i.e., energy gradient (J) and temperature difference (°C), were considered the output response. Table 3 shows that twenty experimental values were incorporated for the optimization study. The central composite design (CCD) was set to operate for 20 runs, split into 14 non-center points (8 factorial design points and 6-star points) and six center points. The values were distributed between $-\alpha = -1.68$ and $\alpha = 1.68$. As shown below, a quadratic equation was adopted to analyze the two output responses. The coded factors equation can be used to predict the response for given levels of each factor. Table 4 shows the fit summary.

Table 3 Actual design parameters

Std. order	Run order	Time of the day	Cooling water type	Flow rate/L min^{-1}	Energy gradient/J	Temperature difference/°C
1	15	− 1	− 1	− 1	13.7	0.8
2	1	1	− 1	− 1	1.7	0.8
3	9	− 1	1	− 1	0.27	0
4	19	1	1	− 1	18	0.04
5	6	− 1	− 1	1	78	0.3
6	7	1	− 1	1	10.5	0.2
7	2	− 1	1	1	11.5	0.04
8	4	1	1	1	27.5	0.04
9	5	− 1.68179	0	0	0	0
10	10	1.68179	0	0	0	0
11	14	0	− 1.68179	0	703	6.8
12	3	0	1.68179	0	630	4
13	20	0	0	− 1.68179	219.5	6.4
14	16	0	0	1.68179	706	6.9
15	13	0	0	0	936.218	6.6
16	12	0	0	0	938.023	6.6
17	17	0	0	0	952.107	6.7
18	8	0	0	0	966.19	6.8
19	18	0	0	0	950.301	6.8
20	11	0	0	0	934.773	6.9

Table 4 Fit summary

Model	Source	Sum of squares	df	Mean square	F-value	p value	
Energy gradient	Quadratic versus 2FI	3.084E + 06	3	1.028E + 06	26.28	< 0.0001	Suggested
Temperature difference	Quadratic versus 2FI	156.03	3	52.01	12.30	0.0011	Suggested

$$-3.35A - 12.4B + 66.78C + 14.15AB - 7.15AC - 6.55BC - 402.44A^2 - 166.8B^2 - 238.84C^2 = 956.66 \quad (1)$$

Table 5 shows that the model has a good fit. It was decided to select the highest-order polynomial where the additional terms are significant, and the model is not aliased. Table 5 shows the significance of the quadratic model used to carry out the optimization. The model statistics are shown in Table 6.

Results and discussion

A volume rate of 0.5 and 1.0 L min^{-1} was measured every 30 s between 08:00 and 17:00 during July 2021 to collect pure water and CuZnS nanofluid as a coolant. This study focused on days in July with the most consistent weather and clear skies. Researchers examined the effects of a PV/T system and a standalone PV on a concentration ratio of CuZnS nanofluid. The average temperature of PV modules is reduced when using coolers, whether purified water or nanofluid mixed with water. Solar irradiation increased throughout the day, causing the temperature gradient panels to climb. Both solar and air radiation have similar patterns; however, PV panels have a significantly more significant surface temperature/radiation factor than cooled panels. Temperature differential and energy gradient have been computed using the relevant sensors' base values. Other temperatures, such as the surface temperature of solar panels, the temperatures of inlets and outlets, and Tedlar, have generally increased due to the rising ambient temperature. In addition, the temperature gradient between the cooling PV panel and the baseline panel decreased during the day; for instance, at noon, the difference was 13 °C, but by the end of the day, it was only 7 °C due to nanofluid obstructing the cooling function. Additionally, several parametric experiments were carried out in this research project.

The crystal structure and chemical name of a substance were found from XRD analysis.

Figure 5a, b shows the XRD pattern for ZnS and ZnS: Cu samples. From the XRD pattern, three prominent peaks corresponding to (1 1 1), (2 2 0) and (3 1 1) reflection planes of ZnS were observed in Fig. 5a. All the diffraction peak positions for the prepared powder are in good accordance with the data reported in JCPDS No. 05-0566 corresponding to the ZnS cubic phase. The peaks were perfectly indexed to the cubic zinc blend phase of ZnS. For ZnS: Cu, along with ZnS peaks (1 1 1), (2 2 0), and (3 1 1) other metallic Cu peaks, with different diffraction peaks appeared at 32.63°, 36.54°, and 61.57° corresponding to (110), (111), (220) planes of cuprite, which indicates the formation of cubic copper (I) oxide nanocrystals. XRD peaks observed for cuprite were matched well with the standard powder diffraction card of bcc (body-centered cubic) cuprite (JCPDS No. 05-667) [36]. The intensity is observed to increase for CuZnS nanocomposites than ZnS particles. The crystallite size of the nanostructured sample

Table 5 ANOVA model

Source	Sum of squares	df	Mean square	F-value	p value	
Model	3.149E+06	9	3.499E+05	8.95	0.0010	Significant
A-Time of the day	153.39	1	153.39	0.0039	0.9513	
B-Cooling water type	2101.26	1	2101.26	0.0537	0.8214	
C-Flow rate	60,906.01	1	60,906.01	1.56	0.2405	
AB	1602.63	1	1602.63	0.0410	0.8436	
AC	409.41	1	409.41	0.0105	0.9205	
BC	342.83	1	342.83	0.0088	0.9273	
A^2	2.334E+06	1	2.334E+06	59.68	< 0.0001	
B^2	4.010E+05	1	4.010E+05	10.25	0.0095	
C^2	8.221E+05	1	8.221E+05	21.02	0.0010	
Residual	3.911E+05	10	39,111.74			
Lack of fit	3.904E+05	5	78,073.82	521.64	< 0.0001	Significant
Pure error	748.34	5	149.67			
Cor total	3.540E+06	19				

Table 6 Statistics of the model

Source	Std. Dev	R^2	Adjusted R^2	Predicted R^2	PRESS	
Energy gradient	197.77	0.8895	0.7901	0.1666	2.951E+06	Suggested
Temperature difference	2.06	0.7905	0.6019	-0.5794	318.65	Suggested

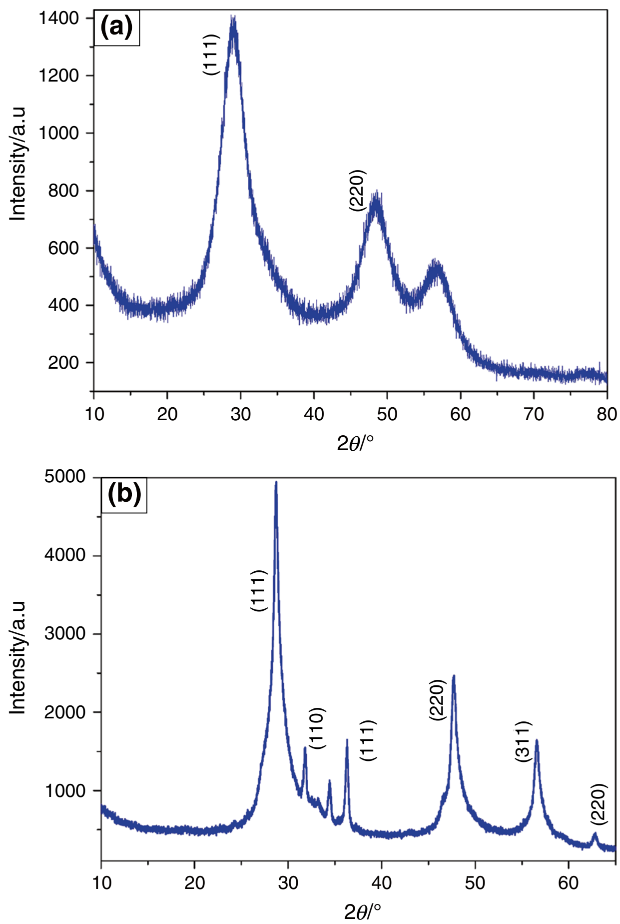

Fig. 5 XRD patterns (**a**) ZnS and (**b**) CuZnS nanocomposites

Table 7 Structural analysis of ZnS and ZnS: Cu nanocomposites

Concentration of ZnS (M)	Grain size (nm)	Dislocation density ($\times 10^{14}$ lines/m^2)	Strain ($\times 10^{-3}$ lines^{2}m^{-4})
0.4	59.35	2.8389	6.0997
ZnS:CuO	17.28	33.44	20.9

is estimated from FWHM (full width at half maximum) of the most intense diffracted line using the Scherrer formula:

$$D = \frac{K\lambda}{\beta \cos\theta} \tag{2}$$

where K is the Scherrer's constant, β is the full width at half maximum. The dislocation density and microstrain of the doped ZnS thin films were calculated using the following equations. The grain size and strain were found to increase with the increase in molarity; the dislocation density decreased with the rise in molarity, as shown in Table 7.

$$\delta = \frac{1}{D^2} \tag{3}$$

$$\varepsilon = \frac{\beta \cos\ \theta}{4} \tag{4}$$

Surface morphological analysis

Figure 6a, b SEM images of ZnS and CuZnS nanocomposites Fig. 6c, d EDAX spectrum of ZnS and CuZnS nanocomposites. Pure ZnS shows a well-packed, crack-free, continuous grain structure without voids [37]. The sample's morphology shows that the image is non-homogenous, with a rough surface where the particles are spherically distributed. Flower-like formation mainly depends on the following steps: initial nucleation and aggregation [38, 39]. ZnS: Cu nanocomposites show a floral-like structure attached to the top of the sheet. The transformation is due to the incorporation of Cu into ZnS. The elemental purity and the element in the prepared samples were examined using energy-dispersive spectroscopy (EDAX). The chemical composition of the prepared nanoparticles was determined by EDAX spectra analysis shown in Fig. 6b, c). The spectra show the presence of Cu, Zn, and S in the samples.

FTIR analysis

Figure 7a, b shows FTIR spectrum of ZnS and CuZnS nanoparticle by co-precipitation method. FTIR transmittance spectra of ZnS and CuZnS nanocomposites synthesized at 80 °C. In FTIR spectra analysis, the transmittance peaks were observed at 612 cm^{-1}, 668 cm^{-1}, 1020 cm^{-1}, 1341 cm^{-1}, 1428 cm-1, 1558 cm^{-1}, 2103 cm^{-1}, and 3301 cm^{-1}. The 612 and 668 cm − 1 peaks are associated with Zn–S vibration and are characteristic of cubic ZnS [40]. The peak at 1559 cm^{-1} is due to a symmetric carboxyl group of Sodium.

The strong transmittance peaks (3400–3465 cm^{-1}) observed for both 3(a, b) spectra have been attributed to the high binding energy of the OH group in the ZnS matrix, and the broad peaks for all ZnS nanoparticles are in the range of 3410–3465 cm^{-1} corresponds to the OH group and also related to the stretching and bending modes of vibration [38]. When the ZnS was doped with Cu^{2+} (spectrum (3b)), the transmittance peaks were at 522 cm^{-1} and 611 cm^{-1} due to Zn–S vibration. A strong peak at 1133 cm^{-1} indicates the presence of the doping ions (Cu^{2+}) in ZnS. Cu nanoparticles had spherical and cubic morphologies and ranged in size from 50 to 100 nm. The findings demonstrated that using Cu–water nanofluids at 0.1 vol% increased thermal conductivity by up to 23.8%.

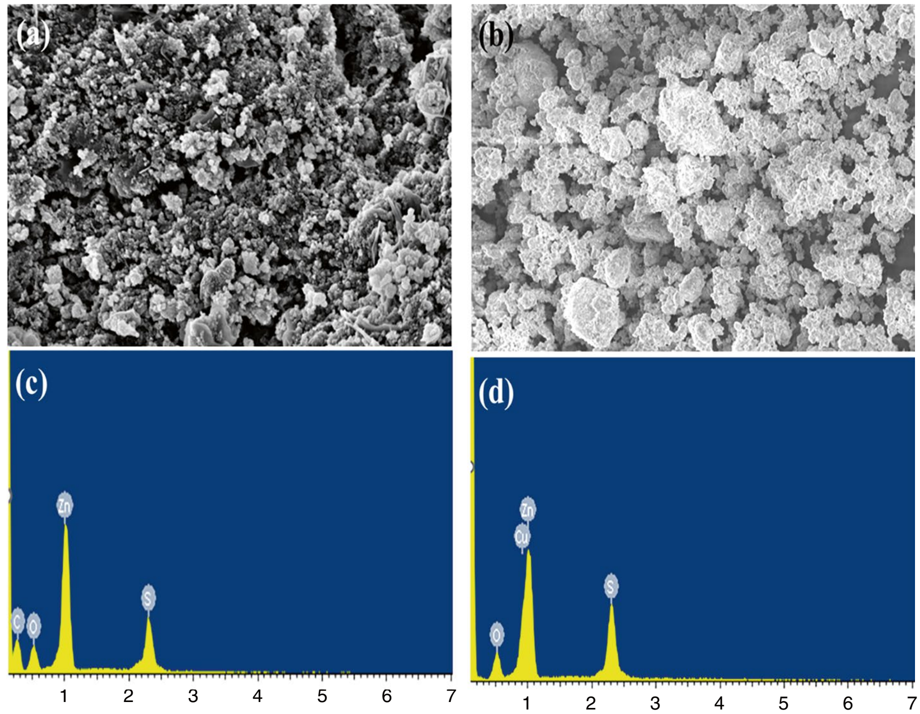

Fig. 6 The SEM analysis (**a**, **b**) of ZnS and CuZnS nanocomposites and the EDAX spectrum (**c**, **d**) of ZnS and CuZnS nanocomposites

Energy gradient in the solar panel

Figures 8–10 show the energy gradient observed in the three different solar panels that were provided with different cooling fluids. The variation in the energy gradient is compared with varying flow rates of the respective cooling fluids. It is observed from Fig. 8 that the energy gradient increased with the flow rate of the plain distilled water. The energy gradient increased by 3.44 times when the flow rate increased to 1.5 L min^{-1} compared to 0.5 L min^{-1}. However, a further increase in flow rate reduced the energy gradient by 27%. It is inferred that solar radiation profoundly influences the energy gradient revealed by the solar panel. The energy gradient peaked near noon, i.e., noon, because of the influencing effect of the heat energy received from the sun at the zenith. The energy gradient for this case was maximum when the distilled water was allowed to flow at two L min^{-1}. It is inferred that the higher flow rate of the distilled water represented a more significant Raynold number that enhanced heat transfer because of convective heat transfer. On the contrary, a lower flow rate, i.e., 0.5 L min^{-1}, contributed to laminar flow. Reddy et al. 2017 [41] in their article mentioned that solar radiation controls the efficiency of the solar panel if the quantity of the cooling fluid is below 0.2 mass%. The efficiency of the solar panel marginally increased by 4% during a trial run.

Figure 9 shows that the energy gradient was lower when the flow rate of the nanofluid, i.e., 0.2 vol. % of ZNS mixed with distilled water, was 0.5 L min^{-1}. This reveals that the nanofluid exhibited natural convective heat transfer, which reduced the energy gradient that occurs through the nanofluid. On the contrary, increasing the flow rate of the ZNS nanofluid to 1.5 L min^{-1} increased the energy gradient by 3.39 folds. This increase in energy gradient is associated with the increase in thermal conductivity and flow rate of the nanofluid. The presence of the additional element in the distilled water enhanced the thermal conductivity, which influenced the energy transfer between the cooling fluid and the solar panel. It is apparent that at higher flow rates significantly enhance the energy gradient and thermal management. Specifically, a flow rate of 2 L min^{-1} achieves the highest energy gradient of around 1000 J, attributed to improved heat transfer efficiency facilitated by the copper zinc sulfide (CuZnS) nanofluid. This optimal flow rate effectively dissipates heat, maintaining lower operational temperatures and enhancing solar panel performance. The findings highlight the potential of using nanofluids, especially CuZnS, to improve the efficiency and durability of solar thermal systems in industrial applications. Hence, water can remove less thermal energy from solar panels when used as a cooling medium, while water-based nanofluids can remove more thermal energy, with flow rate playing a crucial role in producing higher thermal conductivity. Janardhana et al. 2022 [42] revealed that the quantity of nanoparticles affected the efficiency of the solar cells. While using 0.2 mass% of SiO_2 nanofluid, the efficiency increased by 17.8%. However, a further increase in the nanoparticle concentration resulted in a reduction in the efficiency. Ibrahim et al. 2023 [43], during an experiment, showed an increase in the PVT electrical conversion efficiency of 15.5%. A temperature rise

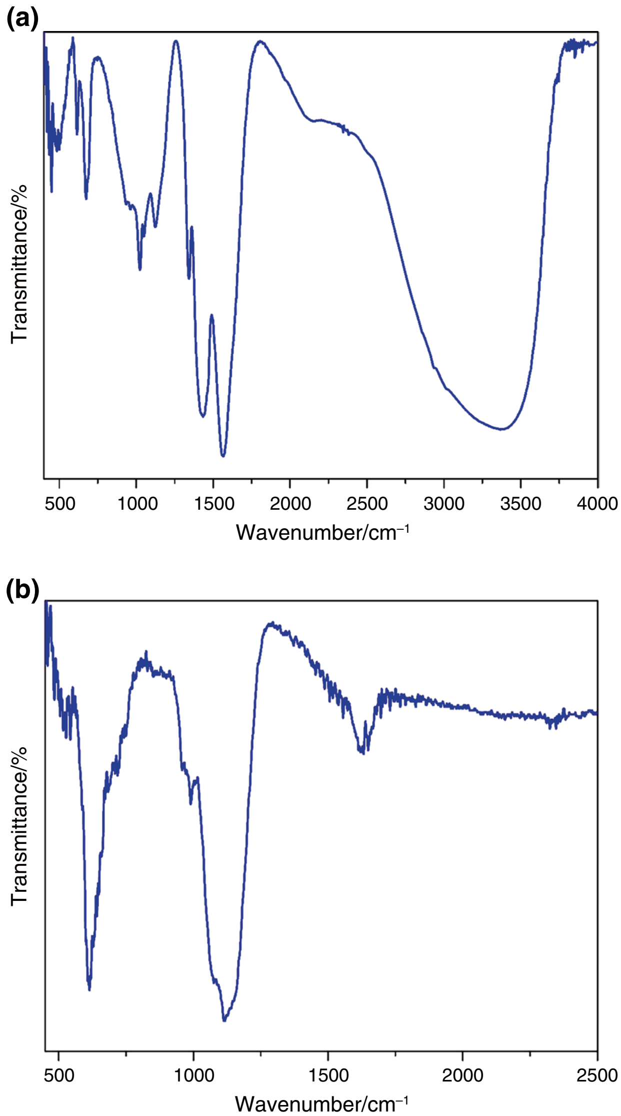

Fig. 7 FTIR spectrum **a** ZnS and **b** CuZnS composites

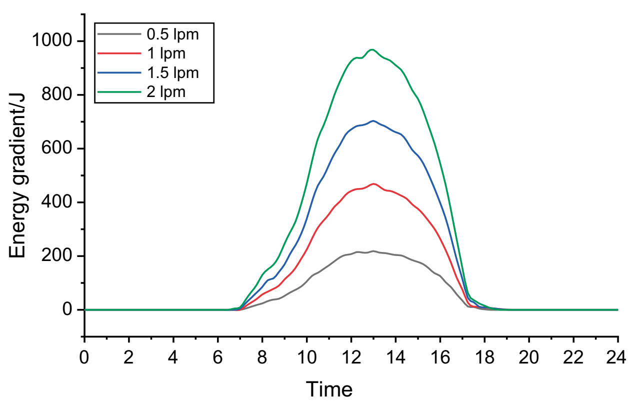

Fig. 8 Energy gradient variation in the solar panel using distilled water

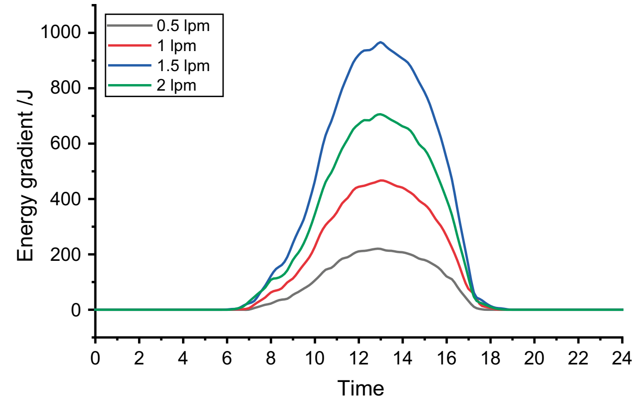

Fig. 9 Energy gradient variation in the solar panel using ZnS nanofluid

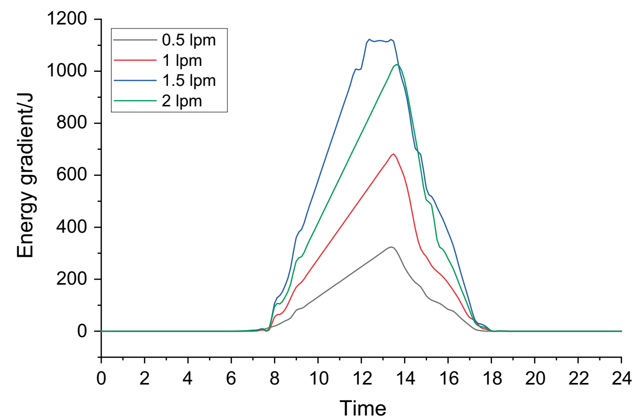

Fig. 10 Energy gradient variation in the solar panel using CuZnS nanofluid

of 22.83% of the surface temperature of PVT panels was observed over the reference panel when the Al_2O_3 volume concentration was 0.05%, and the flow rate was 0.07 kg s^{-1}.

Figure 10 reveals that copper in the nanofluid boosts the heat absorbed from the solar panel. Copper nanoparticles benefit by increasing the thermal conductivity of the cooling fluid. Apart from this, the CuZnS nanoparticles increase the turbulent behavior of the cooling fluid. Because of this, the heat absorbed by the cooling fluid increased. During this case, the energy gradient increased to 1112 W m^{-2}. Similar to the previous case, the maximum energy gradient was observed when the flow rate of CuZnS nanofluid was 1.5 L min^{-1}. The increase in rheological property and the subsequent increase in shear stress of the nanofluid caused a reduced energy gradient while the flow rate was two L min^{-1}. Irrespective of the flow rate, the energy gradient decreased significantly when the solar radiation was reduced during the afternoon. In all cases, the energy gradient remained null without sunlight. A study conducted by Wang et al. 2020

[44] showed that the efficiency of the solar cell increased by 23% while using Sn-doped In_2O_3 doped electron transport layer. A similar study by Logesh et al. 2018 [45] revealed a performance boost of 16.3% while maintaining a flow rate of 2 L min^{-1}.

It is apparent from Fig. 10 that as the flow rate of the nanofluids increases, the energy gradient also rises, with the highest energy gradient observed at a flow rate of 2 L min^{-1}, reaching a peak of approximately 1100 J around the 12th hour. This enhanced performance is primarily due to the increased convective heat transfer efficiency at higher flow rates, which allows for more effective cooling of the solar panel. The steep rise and fall in the energy gradient at higher flow rates suggest a rapid and efficient heat absorption and dissipation cycle, likely driven by the superior thermal properties of the CuZnS nanofluid. This efficient thermal management reduces the operating temperature of the solar panels, thereby enhancing their overall efficiency and longevity. Additionally, the optimal balance between flow rate and heat transfer capabilities at 2 L min^{-1} indicates that further increasing the flow rate may not significantly improve performance due to potential limitations in heat absorption time. This insight is crucial for optimizing solar thermal systems, ensuring they operate within an efficient thermal range while leveraging the advanced properties of nanofluids for enhanced energy collection and conversion.

Temperature difference in the solar panel

Figures 11–13 show the temperature difference observed in the cooling fluid during the experiment. Figure 11 shows the temperature difference when plain distilled water is used as the cooling fluid. The temperature difference was high as soon as the solar energy started heating the solar panel. During this time, the solar panel transitioned from a low-temperature atmosphere to a heated one. Because of this, the temperature difference was noticeable in the cooling fluid. After this duration, the temperature difference remained close, irrespective of the flow rate. The peak temperature difference increased from 6.4 to 7.6 °C when the flow rate of the cooling fluid increased from 0.5 to 1.5 L min^{-1}. After reaching the maximum value, the temperature difference is reduced because of the reduction in available sunlight reaching the solar panel. A study carried out by Santhana Krishnan et al. 2018 [46] revealed that the presence of metal substrate in the nanoparticles increased the thermal conductivity of the nanofluid, resulting in enhancing the efficiency of the solar cells. Shaker et al. 2024 [47] their article informed that the thermodynamic efficiency of the solar panel was reduced from 50 to 43% when the operating temperature increased from 10 to 50 °C, respectively.

Figure 12 shows that the temperature difference was lower when the nanofluid's flow rate, i.e., 0.2 vol. % of ZNS mixed with distilled water, was 0.5 L min^{-1}. This reveals that the nanofluid exhibited natural convective heat transfer, which reduced the Temperature difference occurring through

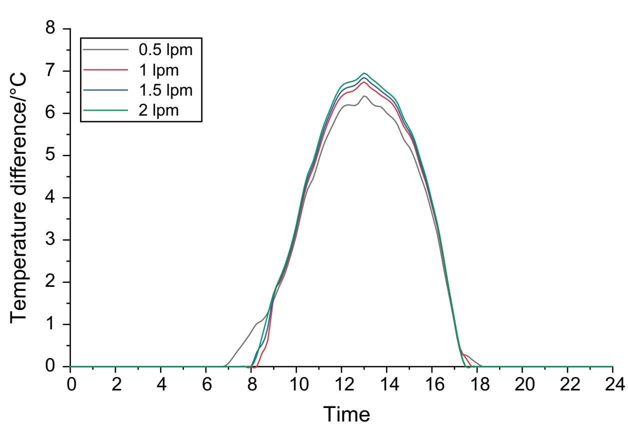

Fig. 11 Temperature variation in solar panel using distilled water

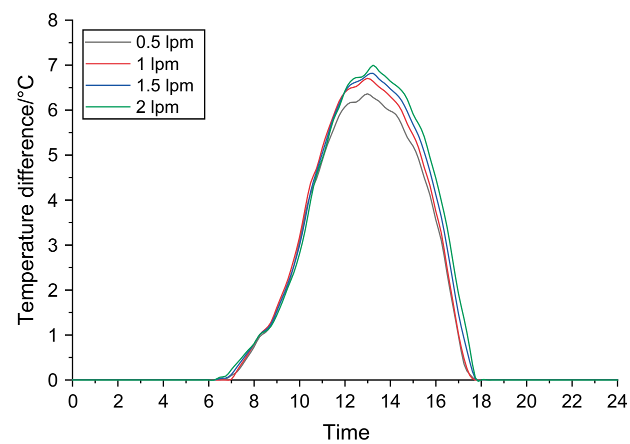

Fig. 12 Temperature variation in the solar panel using ZnS nanofluid

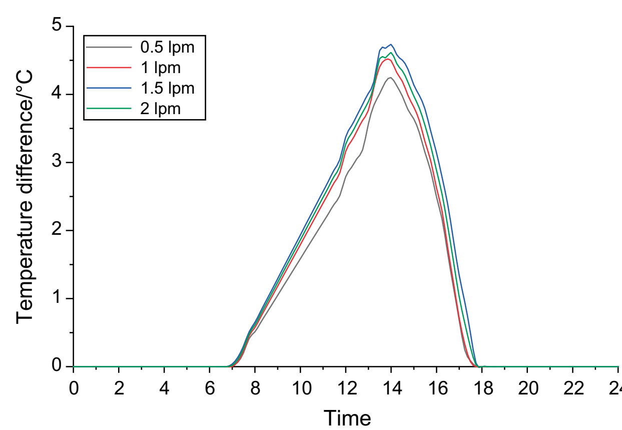

Fig. 13 Temperature variation in solar panel CuZnS nanofluid

the nanofluid. On the contrary, increasing the flow rate of the ZNS nanofluid to 1.5 L min^{-1} increased the Temperature difference by 1%. This increase in temperature difference is associated with the nanofluid's thermal conductivity and flow rate. The presence of the additional element in the distilled water enhanced the thermal conductivity, which influenced the energy transfer between the cooling fluid and the solar panel. It further increased the cooling fluid's flow rate, increasing the nanofluid's rheological behavior. This phenomenon increases the shear stress of the nanofluid, thus leading to a reduction in heat transfer between the solar panel and the cooling fluid.

Figure 13 reveals that copper in the nanofluid boosts the heat absorbed from the solar panel. Copper nanoparticles benefit by increasing the thermal conductivity of the cooling fluid. Apart from this, the CuZnS nanoparticles increase the turbulent behavior of the cooling fluid. Because of this, the heat absorbed by the cooling fluid increased. During this case, the temperature difference increased to 4.73 °C. Similar to the previous case, the maximum Temperature difference was observed when the flow rate of CuZnS nanofluid was 1.5 L min^{-1}. The increase in rheological property and the subsequent increase in shear stress of the nanofluid caused a reduced temperature difference while the flow rate was 2 L min^{-1}. Irrespective of the flow rate, the temperature difference was significantly reduced when the solar radiation was reduced during the afternoon. In all cases, the temperature difference remained null during the absence of sunlight.

Optimization of solar panel

Figure 14 shows the distribution of the energy gradient, while Fig 15 shows the residual vs. run plot. The response values are evenly distributed, and the run values are clustered within the residue.

Figure 16 shows the RSM plots and contour plots for the energy gradient. Figure 16a, b shows that the time of the day significantly influences the energy gradient. The energy gradient was maximum when the day was between 11:00 and 14:00. During this duration, the sun was in the zenith. Figure 16c, d shows that while maintaining a flow rate of 1–1.5 L min^{-1}, the energy gradient was at its peak. Figure 16e, f reveals that the addition of the nanoparticles influences the energy gradient by facilitating enhancement in the thermal conductivity [48]. However, an increase in the flow rate of the cooling water was determinantal to the energy gradient in the solar panel [49]. The energy gradient drops significantly when the flow rate of the cooling water is below 1 L min^{-1}, respectively. A considerable energy gradient was noted when the day was between 08:00 and 17:00. The solar radiation was enormous during the 24:00 test duration.

Figure 17 shows the variation of temperature difference, while Fig. 18 shows the residual vs. run plot for the same

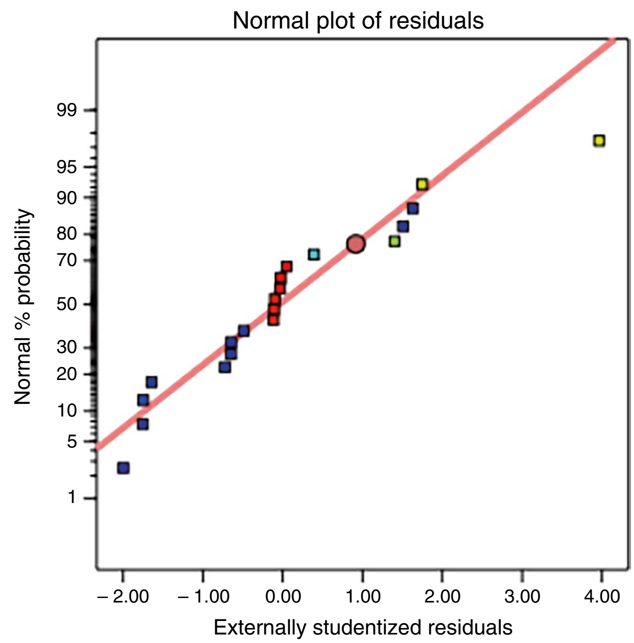

Fig. 14 Typical plot for energy gradient

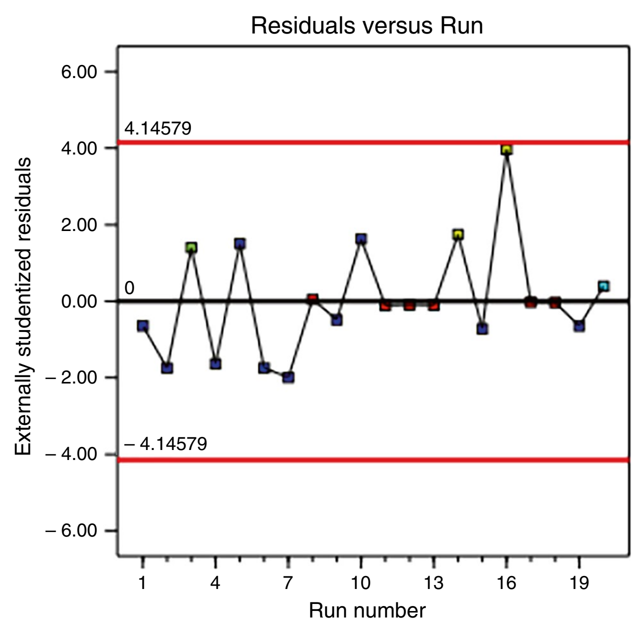

Fig. 15 Residual vs run plot

parameter. The response values are evenly distributed, and the run values are clustered within the residue [50]. Figure 19 shows the RSM plots and contour plots for the temperature difference. Figure 19a, b shows that the time of the day significantly influences the temperature difference. The temperature difference was maximum when the day was between 11:00 and 14:00. During this duration, the sun was in the zenith. Figure 19c, d shows that while maintaining

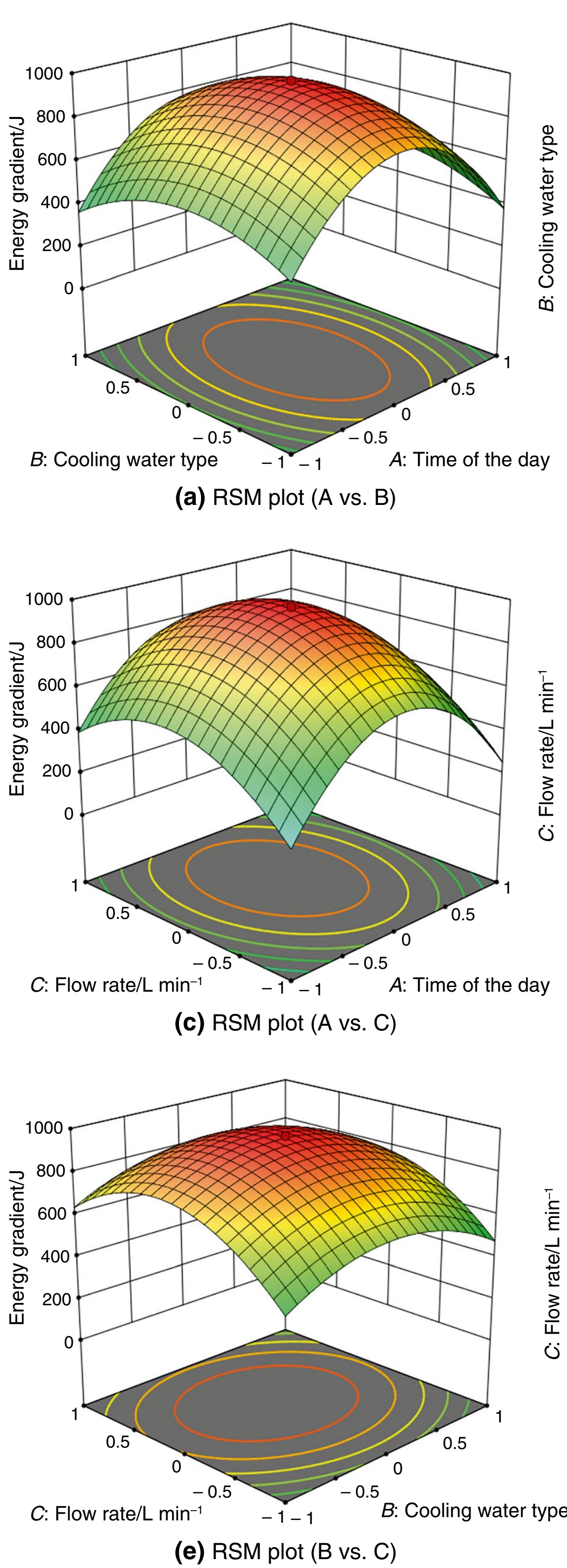

Fig. 16 Response plots for energy gradient

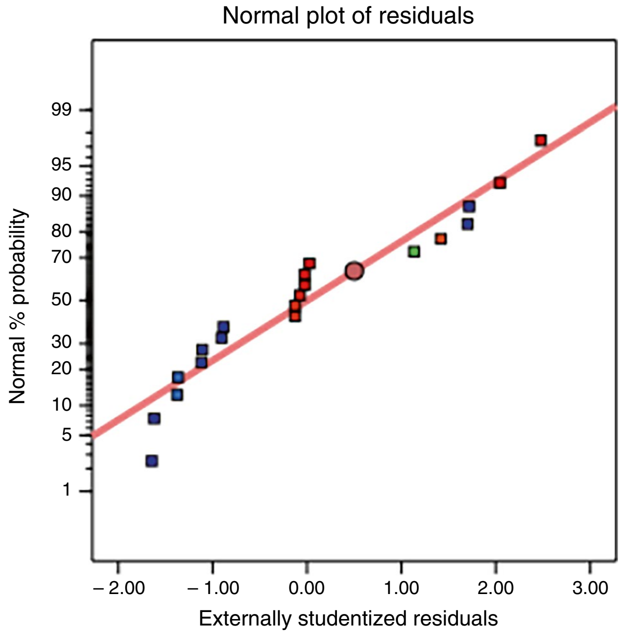

Fig. 17 Typical plot for energy gradient

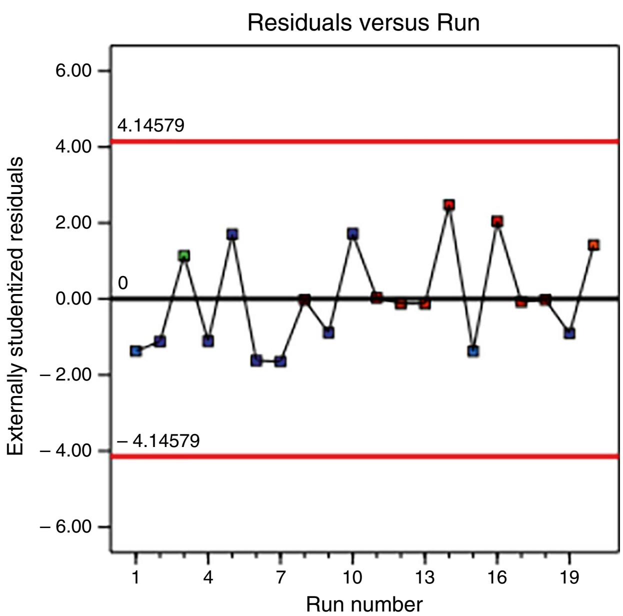

Fig. 18 Residual versus run plot

a flow rate of 1–1.5 L min^{-1}, the temperature difference peaked. Figure 19e, f reveals that the addition of the nanoparticles influences the temperature difference by facilitating enhancement in the thermal conductivity [51]. However, an increase in the flow rate of the cooling water was determinantal to the temperature difference in the solar panel. The temperature difference drops significantly when the flow rate of the cooling water is below 1 L min^{-1}, respectively. A considerable temperature difference was noted when the day was between 08:00 and 17:00. This was when the solar radiation was enormous during the 24:00 test duration. This work addressed three nanofluids with varying flow rates in accordance with the literature reviews, and it generated a number of conclusions that were discussed in the findings and discussion. Nevertheless, compared to previous studies, the volume flow rate would alter as we varied the concentration.

Figure 20 shows the optimization of the response values in the study. It was decided to increase the energy gradient while lowering the temperature difference in the solar panel. According to this set limit, it was revealed that the time of the day should be maximized, and the cooling water type should be enhanced while lowering the flow rate. It is inferred that lowering the flow rate of the cooling fluid reduces the rheological factor occurring in the nanofluid. The addition of copper particles in the nanofluid increases the cooling fluid's thermal conductivity. Hence, it is decided to use CuZnS nanofluid, maintaining a 1.5 L min^{-1} flow rate to enhance the energy gradient while lowering the temperature difference.

Balakrishnan et al. 2023 [52] found that high heating inputs, such as 45W, are beneficial in enhancing the heating period. In contrast, the percentage composition of silicon carbide within the PCM improves the peak temperature of the heat sink and the dwell time of the heat sink. Singh and Yadav 2022 [53] inferred that after optimization in RSM, the best set of input parameters for the solar flux, water inlet velocity, and atmospheric temperature was determined to be 705 W m^{-2}, 0.7263 m s^{-1} of water velocity, and 32.87 °C. Based on these parameters, the response module temperature, the energy efficiency, and the efficiency of the solar panels were 48.98 °C, 19.18%, and 18.88%, respectively. The impact of Al_2O_3 nanofluid and twisted tubes in shell and tube heat exchangers was examined by Ghazanfari et al. in 2023. He had carried out a number of parametric investigations on sun radiation, nanofluid concentration, and baffles with and without them. This led to a 13% pressure decrease and a 25% increase in the heat transfer coefficient [54]. Zhu (2023) examined the effects of PCM being employed on a solar panel system with respect to three different geometries of nanofluid conveying pipes: square, elliptical, and circular. Additionally, they measured the solid PCM volume, liquid PCM volume, and heat transfer rates [55]. The several uses of nanofluid for solar energy harvesting were investigated by Mousavi et al. in 2023 [56]. The adaptive neuro-fuzzy inference system (ANFIS) and the multilayer perceptron (MLP) neural network were the two types of neural networks that Taffarroj et al. studied in order to determine the optimal relationship between the inputs and outputs of the inlet turbulent flow under ultrasonic

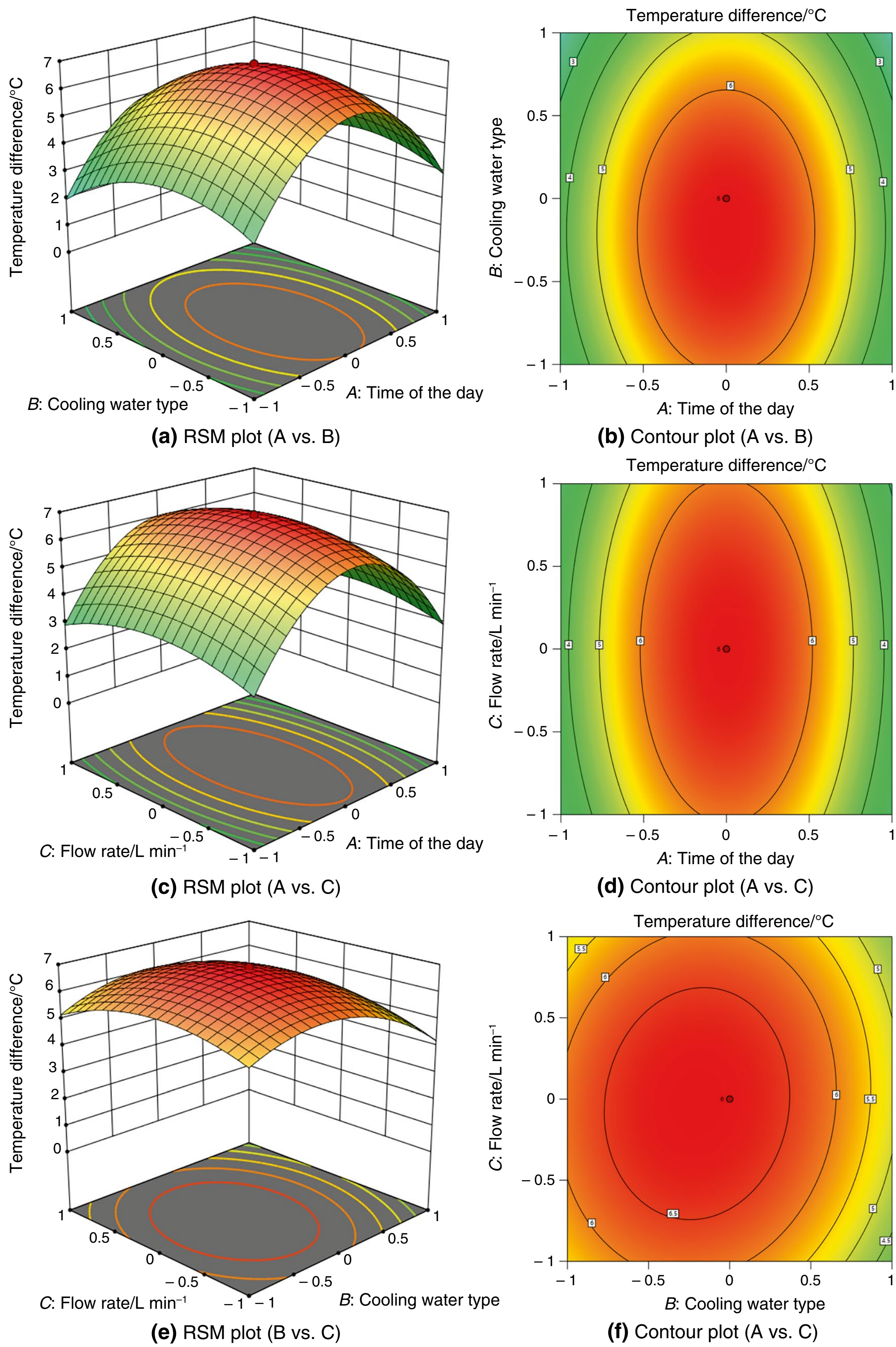

Fig. 19 Response plots for energy gradient

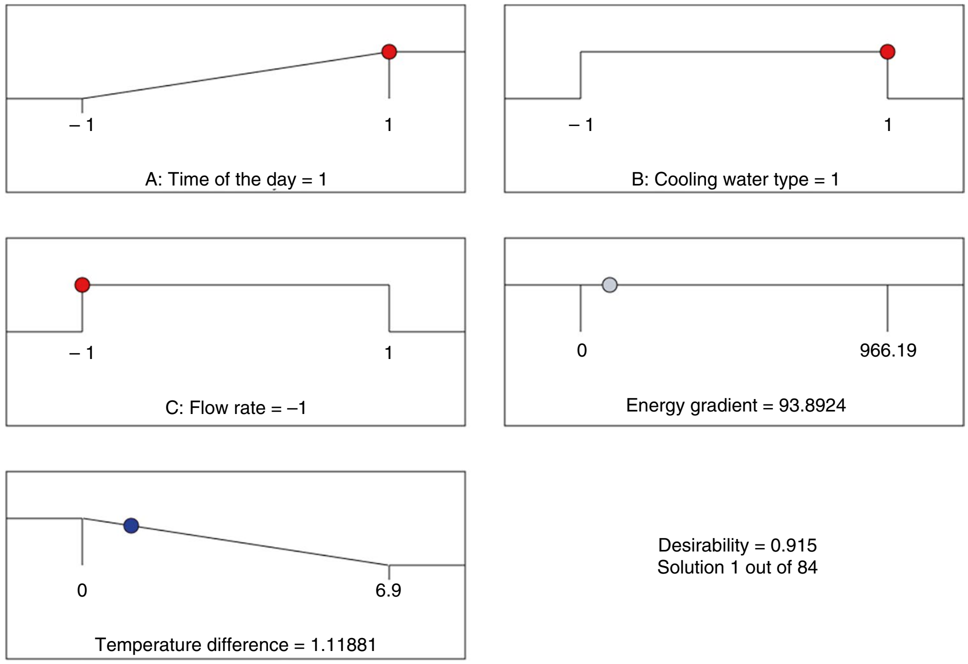

Fig. 20 Optimization of response values

vibration that was extracted from experimental data. The findings indicate that both approaches are successful in forecasting the process's features [57].

Conclusions

This study aimed to ensure uninterrupted operation of a solar panel system by examining the effectiveness of different cooling fluids. Three variants were tested: plain water, water with ZNS, and water with CuZNS, with flow rates set at 0.5 lpm and 1 lpm. The results showed that a flow rate of 1.5 lpm facilitated uniform temperature distribution and consistent heat exchange, crucial for maintaining optimal panel performance. Notably, employing CuZNS nanofluid resulted in lower solar panel temperatures due to enhanced heat exchange capabilities. The recorded data over a 24-h period provided insights into temperature fluctuations and informed the optimization of energy gradient and temperature difference parameters. Remarkably, using CuZnS nanofluid at 1.5 L min^{-1} yielded a significant increase in energy gradient, reaching a maximum of 1112 W m^{-2}. This enhancement can be attributed to the heightened thermal conductivity of the nanofluid, owing to the presence of copper particles. Consequently, it is recommended to utilize CuZnS nanofluid at a flow rate of 1.5 L min^{-1} to achieve optimal performance by maximizing energy gradient while minimizing temperature differences in the solar panel system.

Scope of future research

The study also focuses on short-term performance, potentially overlooking the long-term stability and degradation of nanofluids. Additionally, environmental factors such as varying sunlight intensity and ambient temperatures were not extensively considered, which could impact real-world applicability. Future research could address these limitations by exploring a wider range of flow rates, conducting long-term stability studies, and incorporating diverse environmental conditions. Investigating the cost-effectiveness and practical implementation challenges of CuZnS nanofluids, as well as comparing them with other advanced cooling technologies, could further enhance the understanding and application of these findings.

Author contributions M. Arulprakasajothi and A. Saranya were responsible for the conceptualization and methodology of the study. Srimanickam contributed to the review and editing of the manuscript. Yuvarajan Devarajan provided supervision and was also responsible for visualization. N. Dilip Raja handled data curation and offered additional supervision.

Funding Not applicable.

Data availability The datasets used and/or analyzed during the current study available from the corresponding author on reasonable request.

Code availability Not applicable.

Declarations

Conflict of interest Not applicable.

Ethics approval Not applicable.

Consent to participate Not applicable.

Consent for publication Not applicable.

References

1. Monika, G., Melanie Kim, S. R., Kumar, P. S., Gayathri, K. V., Rangasamy, G., & Saravanan, A. (2023). Biofortification: A long-term solution to improve global health- a review. Chemosphere, 314, 137713. https://doi.org/10.1016/j.chemosphere.2022.137713
2. Arulprakasajothi M, Poyyamozhi N, Chandrakumar P, Dilip Raja N, Yuvarajan D. Experimental investigation of salinity gradient solar pond with nano-based phase change materials. Energy Sour, Part A: Recovery, Utilisation, Environ Eff. 2023;45(2):5465–80. https://doi.org/10.1080/15567036.2023.2207508.
3. Muthu G, Thulasi S, Dhinakaran V, Mothilal T. Performance of solar parabolic dish thermoelectric generator with PCM. Mater Today: Proc. 2021;37:929–33. https://doi.org/10.1016/j.matpr.2020.06.123.
4. JafarKutbudeen S, Arulprakasajothi M, N., B., & Elangovan, K. Effect of conical strip inserts in a parabolic trough solar collector under turbulent flow. Energy Sour, Part A: Recovery, Utilisation, Environ Eff. 2019;44(1):2556–68. https://doi.org/10.1080/15567036.2019.1650850.
5. Arulprakasajothi M, Dilip Raja N, BeemKumar Elangovan NK. Experimental study on Al2O3 /H2O nanofluid with conical sectional insert in concentric tube heat exchanger. Energy Sour, Part A: Recovery, Utilisation, Environ Eff. 2019;44(1):2402–14. https://doi.org/10.1080/15567036.2019.1649753.
6. Mishra S, Swain K, Dalai R. Heat and mass transfer of water-based copper and alumina hybrid nanofluid over a stretching sheet. Heat Transfer. 2022;52(2):1198–214.
7. NematpourKeshteli A, Iasiello M, Langella G, Bianco N. Enhancing PCMs thermal conductivity: a comparison among porous metal foams, nanoparticles and finned surfaces in triplex tube heat exchangers. Appl Therm Eng. 2022;212: 118623. https://doi.org/10.1016/j.applthermaleng.2022.118623.
8. Mertaslan OM, Keklikcioglu O. Investigation the effect of concurrent implementation of hybrid nanofluid and modified inserts on thermohydraulic performance of a heat exchanger tube. Heat Transf Res. 2024;55(1):69–84. https://doi.org/10.1615/heattransres.2023048985.
9. Oflaz F, Keklikcioglu O, Ozceyhan V. Investigating thermal performance of combined use of SiO2-water nanofluid and newly designed conical wire inserts. Case Stud Therm Eng. 2022;38: 102378. https://doi.org/10.1016/j.csite.2022.102378.
10. Shajahan MI, Stephen C, Michael JJ, Arulprakasajothi M, Rathnakumar P, Parthasarathy M. Heat transfer investigations of in-line conical strip inserts using MWCNT/water nanofluid under laminar flow condition. Int J Therm Sci. 2023;183: 107844. https://doi.org/10.1016/j.ijthermalsci.2022.107844.
11. Kahveci M, Koca T. Experimental study of effect of using graphene oxide-water-based nanofluids in plate heat exchanger on thermal performance. Heat Transf Res. 2023;54(15):57–70. https://doi.org/10.1615/heattransres.2023046711.
12. El Alami Y, Lamkaddem A, Bendaoud R, Talbi S, Baghaz E. Numerical study of a water-based photovoltaic-thermal (PVT) hybrid solar collector with a new heat exchanger. e-Prime-Advances Electrical Eng Electronics Energy. 2024. https://doi.org/10.1016/j.prime.2024.100693.
13. Muniyandi S, Narayanasamy S. Experimental analysis on the performance of photovoltaic module with Al2O3 deionized water nanofluid. Therm Sci. 2024. https://doi.org/10.2298/tsci230829268m.
14. Madas SR, Narayanan R, Gudimetla P. Numerical investigation on the optimum performance output of photovoltaic thermal (PVT) systems using nano-copper oxide (CuO) coolant. Sol Energy. 2023;255:222–35. https://doi.org/10.1016/j.solener.2023.02.035.
15. Kazem HA, Al-Waeli AHA, Chaichan MT, Sopian K. Numerical and experimental evaluation of nanofluids based photovoltaic/thermal systems in Oman: Using silicone-carbide nanoparticles with water-ethylene glycol mixture. Case Stud Therm Eng. 2021;26: 101009. https://doi.org/10.1016/j.csite.2021.101009.
16. Bassam AM, Sopian K, Ibrahim A, Al-Aasam AB, Dayer M. Experimental analysis of photovoltaic thermal collector (PVT) with nano PCM and micro-fins tube counterclockwise twisted tape nanofluid. Case Stud Therm Eng. 2023;45: 102883. https://doi.org/10.1016/j.csite.2023.102883.
17. Sheikholeslami M, Khalili Z. Investigation of solar Photovoltaic cell utilizing hybrid nanofluid confined jet and helical fins for improving electrical efficiency in existence of thermoelectric module. Appl Therm Eng. 2023;234: 121329. https://doi.org/10.1016/j.applthermaleng.2023.121329.
18. Al-Waeli AHA, Sopian K, Kazem HA, Chaichan MT. Photovoltaic Thermal (PV/T). Photovoltaic Therm Collectors Nanofluids Nano-PCM. 2024. https://doi.org/10.1007/978-981-99-9126-6_1.
19. Sami. Analysis of Solar Absorption Chiller driven by CuO Nanofluid-based PV- Thermal Solar collectors (PVT). Int J Therm Eng. 2024;10(1):1–10.
20. Kouravand A, Kasaeian A, Pourfayaz F, Vaziri Rad MA. Evaluation of a nanofluid-based concentrating photovoltaic thermal system integrated with finned PCM heatsink: an experimental study. Renew Energy. 2022;201:1010–25. https://doi.org/10.1016/j.renene.2022.11.025.
21. Chen Y, Meng Y, Zhang J. Leakage proof, flame-retardant, and electromagnetic shield wood morphology genetic composite phase change materials for solar thermal energy harvesting. Nano-Micro Lett. 2024;16:196. https://doi.org/10.1007/s40820-024-01414-4.
22. Ghazanfari V, Taheri A, Amini Y, Mansourzade F. Enhancing heat transfer in a heat exchanger: CFD study of twisted tube and nanofluid (Al2O3, Cu, CuO, and TiO2) effects. Case Stud Therm Eng. 2024;1(53): 103864. https://doi.org/10.1016/j.csite.2023.103864.
23. Arash K, Meysam K, Maadi RS, Ma T. Performance optimisation of a nanofluid-based photovoltaic thermal system integrated with nano-enhanced phase change material. Appl Energy. 2021. https://doi.org/10.1016/J.APENERGY.2021.116859.
24. Fazlay R, Likhan D, Khairul H, Navid A, Rahman S, Rahman S, Tauhidur R. State-of-the-art review on water-based nanofluids for low temperature solar thermal collector application. Solar Energy Mater Solar Panels. 2021. https://doi.org/10.1016/J.SOLMAT.2021.111220.
25. A.H., Saleh., Adnan, M., Hussein., Suad, Hassan, Danook. (2021). Efficiency enhancement of solar panel collector using Fe3O4/water nanofluid In IOP Conference Series: Materials Science and Engineering https://doi.org/10.1088/1757-899X/1105/1/012059
26. Majdi Mashkour Habeeb Sabry HSAMLJAH. Enhancement of energy transfer efficiency for photovoltaic (PV) systems by cooling the panel surfaces. Eastern-European J Enterprise Technologies. 2021;4:83–9. https://doi.org/10.15587/1729-4061.2021.238700.

27. Kandeal Algazzar Elkadeem ThakurAbdelaziz El-Said Elsaid An AWMAMRAKGB EMAMM, Kandel FawzySharshir R HESW. Nano-enhanced cooling techniques for photovoltaic panels: a systematic review and prospect recommendations. Sol Energy. 2021;227:259–72. https://doi.org/10.1016/J.SOLENER.2021.09.013.
28. Bhakre Sawarkar Kalamkar SSDPVR. Performance evaluation of PV panel surfaces exposed to hydraulic cooling–A review. Sol Energy. 2021;224:1193–209. https://doi.org/10.1016/J.SOLENER.2021.06.083.
29. Özakin AN, Kaya F. Effect on the exergy of the PVT system of fins added to an air-cooled channel: a study on temperature and air velocity with ANSYS Fluent. Sol Energy. 2019;184:561–9.
30. Hernandez-Perez Carrillo Bassam Flota-Bañuelos Patiño-Lopez JGJGAMLD. A new passive PV heatsink design to reduce efficiency losses: a computational and experimental evaluation. Renew Energy. 2020;147:1209–20. https://doi.org/10.1016/J.RENENE.2019.09.088.
31. Diyang C, Shunlin L, Dongdong W, Zheng L. A 1 km global dataset of historical (1979–2013) and future (2020–2100) Köppen-Geiger climate classification and bioclimatic variables. Earth Syst Sci Data. 2021;13(11):5087–114. https://doi.org/10.5194/ESSD-13-5087-2021.
32. Sathishkumar M, Saroja M, Venkatachalam M. Influence of (Cu, Al) doping concentration on the structural, optical and antimicrobial activity of ZnS thin films prepared by Sol-Gel dip coating techniques. Optik. 2019;182:774. https://doi.org/10.1016/j.ijleo.2019.02.014.
33. Pan P, Lihui Chen Yu, Jun DD, Feng C, Zhengbing Fu, Caiqin Q, Wang F. Nitrogen-doped carbon decorated Cu2NiSnS4 microflowers as superior anode materials for long-life lithium-ion batteries. J Solid State Chem. 2018;261:103–10.
34. Alwany A, Alnakhlani A, Youssef G, Algradee M, Hassan B. Effect of Li+ concentration on the structural and optical properties of chemically synthesised ZnS nanoparticles. Results Optics. 2023;12: 100424. https://doi.org/10.1016/j.rio.2023.100424.
35. Mohamed Riyas Z, Ramesh Prabhu M, Sankaranarayanan K. Hydrothermal synthesis of La_2O_3–ZnO nanocomposites as electrode material for asymmetric supercapacitor applications. J Mater Sci: Mater Electron. 2023;34:1612. https://doi.org/10.1007/s10854-023-10988-5.
36. Amiri Delouei A, Naeimi H, Sajjadi H, Atashafrooz M, Imanparast M, Chamkha AJ. An active approach to heat transfer enhancement in indirect heaters of city gate stations: an experimental modeling. Appl Therm Eng. 2024;237: 121795. https://doi.org/10.1016/j.applthermaleng.2023.121795.
37. Hedeshi M, Jalali A, Arabkoohsar A, Amiri Delouei A. Nanofluid as the working fluid of an ultrasonic-assisted double-pipe counter-flow heat exchanger. J Therm Anal Calorim. 2023;148(16):8579–91. https://doi.org/10.1007/s10973-023-12102-7.
38. Delouei AA, Sajjadi H, Ahmadi G. The effect of piezoelectric transducer location on heat transfer enhancement of an ultrasonic-assisted liquid-cooled CPU radiator. Iranian J Sci Technol Transactions Mechanical Eng. 2023;48(1):239–52. https://doi.org/10.1007/s40997-023-00667-5.
39. Amiri Delouei A, Sajjadi H, Atashafrooz M, Hesari M, Ben Hamida MB, Arabkoohsar A. Louvered fin-and-flat tube compact heat exchanger under ultrasonic excitation. Fire. 2022;6(1):13. https://doi.org/10.3390/fire6010013.
40. Amiri Delouei A, Sajjadi H, Ahmadi G. Ultrasonic vibration technology to improve the thermal performance of CPU water-cooling systems: experimental investigation. Water. 2022;14(24):4000. https://doi.org/10.3390/w14244000.
41. Janardhana K, Sivakumar A, Suresh R, Ramesh C, Musthafa AS, Vishwakarma S. Analysing thermal performance of a solar PV using a nanofluid. Mater Today Proc. 2022. https://doi.org/10.1016/j.matpr.2022.08.177.
42. Ibrahim A, Ramadan MR, Khallaf AEM, Abdulhamid M. A comprehensive study for Al2O3 nanofluid cooling effect on the electrical and thermal properties of polycrystalline solar panels in outdoor conditions. Environ Sci Pollut Res. 2023;30(49):106838–59. https://doi.org/10.1007/s11356-023-25928-3.
43. Wang P, et al. Gradient energy alignment engineering for planar perovskite solar cells with efficiency over 23%. Adv Mater. 2020;32(6):1–8. https://doi.org/10.1002/adma.201905766.
44. Logesh K, Arulprakasajothi M, Rohith Renish R, Venkatasudhahar M, Dilip Raja N. Impact of water-based TiO2 nanofluid on heat transfer under transition flow. Mater Today Proc. 2018. https://doi.org/10.1016/j.matpr.2018.06.432.
45. Santhana Krishnan R, Arulprakasajothi M, Logesh K, Dilip Raja N, Rajendra M. Analysis and feasibilty of nano-lubricant in vapour compression refrigeration system. Mater Today Proc. 2018. https://doi.org/10.1016/j.matpr.2018.06.437.
46. Shaker LM, Al-Amiery AA, Hanoon MM, Al-Azzawi WK, Kadhum AAH. Examining the influence of thermal effects on solar cells: a comprehensive review. Sustain Energy Res. 2024. https://doi.org/10.1186/s40807-024-00100-8.
47. Jafer Kutbudeen S, Logesh K, Mahalingam A, Vinoth kanna A. Performance enhancement of solar collector using strip inserts and with water based Al2O3/DI water nanofluids. Energy Sources, Part A Recover Util Environ Eff,. 2021. https://doi.org/10.1080/15567036.2021.1872745.
48. Esfandyari M, Amiri Delouei A, Jalai A. Optimization of ultrasonic-excited double-pipe heat exchanger with machine learning and PSO. Int Commun Heat Mass Transf. 2023;147: 106985. https://doi.org/10.1016/j.icheatmasstransfer.2023.106985.
49. Rezaei P, Moheghi HR, Amiri Delouei A. Design and optimization of a spiral-tube instantaneous water heater using response surface methodology. Water. 2023;15(8):1458. https://doi.org/10.3390/w15081458.
50. Khajezade Roodi M, Jalali A, Hedayati A, Amiri Delouei A. Optimization of spark ignition engine performance using a new double intake manifold: experimental and numerical analysis. J Appl Computational Mech. 2023;9(1):1–14. https://doi.org/10.22055/jacm.2020.34234.2365.
51. Sajjadi H, Nabavi SN, Atashafrooz M, Amiri Delouei A. Optimization of heating and cooling system locations by taguchi's method to maximize or minimize the natural convection heat transfer rate in a room. Iranian J Sci Technol, Transactions Mechanical Eng. 2023;47(4):1599–614. https://doi.org/10.1007/s40997-023-00624-2.
52. Singh V, Yadav VS. Optimising the performance of solar panel cooling apparatus by application of response surface methodology. Proc Inst Mech Eng Part C J Mech Eng Sci. 2022. https://doi.org/10.1177/09544062221101828.
53. Ghazanfari V, Imani M, Shadman MM, Amini Y, Zahakifar F. Numerical study on the thermal performance of the shell and tube heat exchanger using twisted tubes and Al2O3 nanoparticles. Prog Nucl Energy. 2023;1(155): 104526.
54. Zhu C. Optimizing and using AI to study of the cross-section of finned tubes for nanofluid-conveying in solar panel cooling with phase change materials. Eng Anal Boundary Elem. 2023;1(157):71–81.
55. Mousavi SM, Alborzi ZS, Raveshiyan S, Amini Y. Applications of nanotechnology in the harvesting of solar energy. Nanotechnol Applications Solar Energy Syst. 2023;30:239–56.

56. Tafarroj MM, Amiri Delouei A, Hajjar A, Ben Hamida MB, Izadi M. MLP and optimized FCM-ANFIS models proposed for inlet turbulent flow under ultrasonic vibration. J Therm Anal Calorim. 2023;148(24):13995–4009.
57. Bandrehalli Chandrashekaraiah M, Nagappan B, and Devarajan Y. Hybrid power generation: Experimental investigation of PCM and TEG integration with photovoltaic systems. Int Res J Multidiscip Techno 2024;225–231. https://doi.org/10.54392/irjmt24317